ACS OMEGA

http://pubs.acs.org/journal/acsodf

Article

γ-Irradiated Chitosan Mediates Enhanced Synthesis and Antimicrobial Properties of Chitosan−Silver (Ag) Nanocomposites

Shriram Mirajkar, Prakash Rathod, Bharat Pawar, Suprasanna Penna, and Sunil Dalvi*

Cite This: *ACS Omega* 2021, 6, 34812−34822

Read Online

ACCESS | Metrics & More | Article Recommendations | Supporting Information

ABSTRACT: Chitosan (CSN) and its derivatives are being exploited for their potential role in agriculture in mitigating environmental stress factors. The present study was aimed to enhance the synthesis of chitosan (CSN)-based silver nanoparticles (Ag NPs) using γ-irradiated chitosan (IR-CSN) and to study the antimicrobial activity of IR-CSN−Ag NPs. The chitosan−silver nanocomposites (CSN−Ag NPs) were prepared by employing the green synthesis method using normal chitosan (high molecular weight (MW), NL-CSN) and oligochitosans (low MW, IR-CSN). The latter was derived by irradiation with γ rays (^{60}Co) at 100 kGy dose to obtain a lower MW (approximately 25 kDa). NL-CSN and IR-CSN (0.0−2.5% w/v) were amalgamated with different concentrations of silver nitrate (0.0−2.5% w/v) and vice versa. The UV−visible spectra displayed a single peak in the range of 419−423 nm, which is the characteristic surface plasmon resonance (SPR) for Ag NPs. The physicochemical properties were assessed using different methods such as transmission electron microscopy (TEM), Fourier transform infrared (FTIR), zetasizer, elemental (CHNS) analysis, etc. The degree of Ag NP synthesis was more in IR-CSN than NL-CSN. The *in vitro* disc diffusion assay with IR-CSN−Ag NPs exhibited a significantly higher antimicrobial activity against *Escherichia coli*. Further evaluation of the antifungal activity of IR-CSN and Ag NPs showed a synergistic effect against chickpea wilt (*Fusarium oxysporum* f. sp. *ciceris*). The study has provided a novel approach for the improved synthesis of CSN−Ag nanoparticle composites using γ-irradiated chitosan. This study also opens up new options for the development and deployment of γ-irradiated chitosan−silver nanocomposites for the control of phytopathogens in sustainable agriculture.

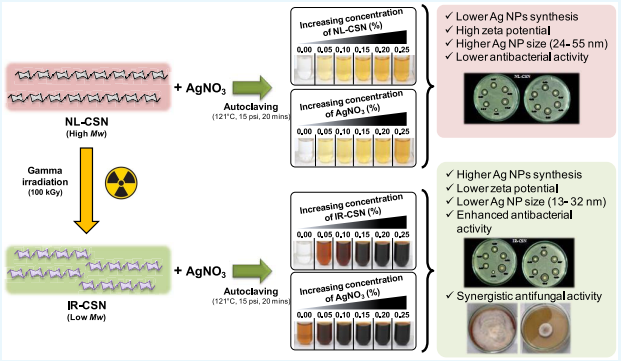

1. INTRODUCTION

There is a growing interest in the use of chitosan (CSN) and its derivatives for a wide spectrum of applications, ranging from agriculture to environment to healthcare.[1−3] Chitosan, derived by deacetylation of chitin, is considered as one of the most abundant biopolymers, next to cellulose, and is well known for its nontoxic, nonallergenic, biodegradable, and biocompatible properties.[4] Chitosans are binary copolymers composed of *N*-acetyl-D-glucosamine and D-glucosamine monomeric residues. Differences in the degree of deacetylation (DD), pattern of acetylation (PA), and molecular weight (MW) impart diversity to chitosan, which has a direct impact on its biological properties.[5,6]

Chitosan and its derivatives have been immensely exploited as versatile bioactive substances because of their superior material and functional properties. Biological effects of chitosan include antimicrobial (against bacteria, fungi, and viruses) and antioxidant (to encounter oxidative damages caused due to adverse conditions) activities.[6,7] One of the limitations in the exploitation of various biological properties of chitosan is its insolubility in water, which greatly limits its application in various fields. It has also been shown that reduction in polymer length and overall molecular weight (MW) results in enhanced biological activity of chitosans. Among the different methods employed to reduce the MW of chitosan polymers, γ irradiation has proven to be the most appropriate for modifying the physical and chemical properties of the chitosan polymer to improve its solubility (by reducing its MW), antimicrobial and antioxidant properties, as well as plant-growth-promoting properties.[8−12]

In our earlier efforts to optimize the γ-irradiation doses, we found that a 100 kGy dose was sufficient to obtain degraded low-MW oligochitosan (IR-CSN) polymers bearing superior biological properties.[11−14] Use of a 100 kGy γ-radiation dose for effective degradation of chitosan has been advocated previously by Choi et al.[8] The IR-CSN has been tested for various physicochemical characteristics as well as enhanced biological properties such as against biotic (antifungal) and

Received: September 27, 2021
Accepted: November 30, 2021
Published: December 10, 2021

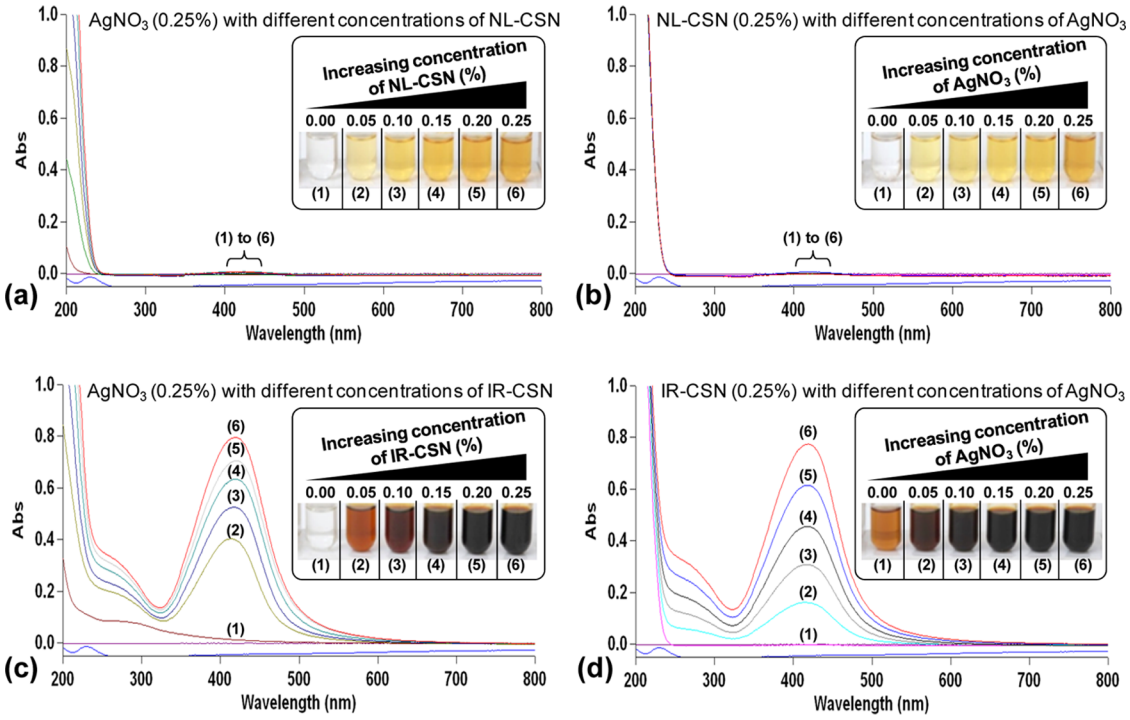

Figure 1. UV−visible spectroscopy observations showing that surface plasmon resonance (SPR) of Ag NP increased with increasing concentrations of chitosan and $AgNO_3$ in both NL-CSN (a, b) and IR-CSN (c, d). The change in color intensity was a primary indicator of the formation of Ag nanoparticles.

abiotic stress (water deficit) tolerance, as well as antioxidant and growth-promoting properties in crop plants of potato, sugarcane, pea, onion, etc.[11−16]

Synthesis and use of metal nanoparticles (NPs) and nanomaterials have gained significant attention during recent decades. Among others, silver nanoparticles (Ag NPs) have received special attention not only in research but also for industrial applications because of their potential chemical and biological properties.[17,18] Various physical and chemical methods (such as γ-irradiation, sonochemical and microwave-assisted, laser ablation, thermal decomposition, lithography, polyol and chemical reduction, etc.) can be employed for the synthesis of silver nanoparticles.[19] Most of these chemical methods involve the use of reducing and stabilizing agents, which are toxic and lead to formation of nonbiodegradable products with environmental toxicity. In this regard, alternative approaches of green synthesis methods have emerged as cost-effective, nontoxic, environmental-friendly, and amenable for scale-up for mass synthesis and do not need the use of toxic chemicals.[20]

In recent years, there has been great interest in enhancing antimicrobial and plant-growth-promoting properties by chemical modification of chitosan and creating composite materials with other antibacterial materials to improve their efficacy and stability.[21] In the recent past, synthesis of chitosan−metal nanocomposites by various (chemical or physical) methods has become a major focus to further improve the antimicrobial activity of chitosans. Significant enhancement in antibacterial and antifungal activities of chitosan−silver nanocomposites (in different forms such as aqueous solutions, films, microspheres, etc.) has been achieved against various potential microbial species (*Staphylococcus aureus*, *Escherichia coli*, *Rhizopus*, *Mucor*, and others) compared to either of silver nanoparticles or chitosan alone.[6,22] Among the different methods employed to synthesize chitosan−silver nanocomposites, use of γ-irradiation for reduction of silver ions in solution in the presence of chitosan has been reported previously.[23−25] However, there are no studies on the use of γ-irradiated chitosan for the synthesis of silver nanoparticles for antimicrobial applications.

In the present study, we performed a comparative investigation on the synthesis and characterization of chitosan−silver nanocomposite particles (CSN−Ag NPs) by the green synthesis (thermal reduction) method using a high-MW (normal CSN (NL-CSN)) chitosan and its γ-irradiated (low MW, IR-CSN) oligochitosan derivative. To the best of our knowledge, this is the first report wherein the chitosan−Ag NPs were synthesized through the green synthesis method using γ-irradiated (low MW, IR-CSN) oligochitosan and evaluated to exhibit better physicochemical characteristics along with enhanced antimicrobial activity compared to nonirradiated (high MW, NL-CSN) chitosan.

2. RESULTS AND DISCUSSION

The present study was performed to investigate the possible differential effects on the use of normal high-MW chitosan (NL-CSN) and γ-irradiated low-MW oligochitosan (IR-CSN) on the synthesis of Ag NPs using the green method. The present approach is contrary to earlier reports wherein γ-radiation was utilized to synthesize chitosan−Ag nanoparticles.[23−25] In these earlier reports, γ-radiation-mediated degradation of chitosan was not considered, which indeed is an important factor as the fragmentation of the chitosan polymer influences Ag NP synthesis. In the present study, γ-irradiated chitosan has been used for the synthesis of chitosan−silver nanocomposites.

2.1. Synergistic Effect of Chitosan and $AgNO_3$ Concentration on Synthesis of Ag NPs. Change in color

https://doi.org/10.1021/acsomega.1c05358
ACS Omega 2021, 6, 34812−34822

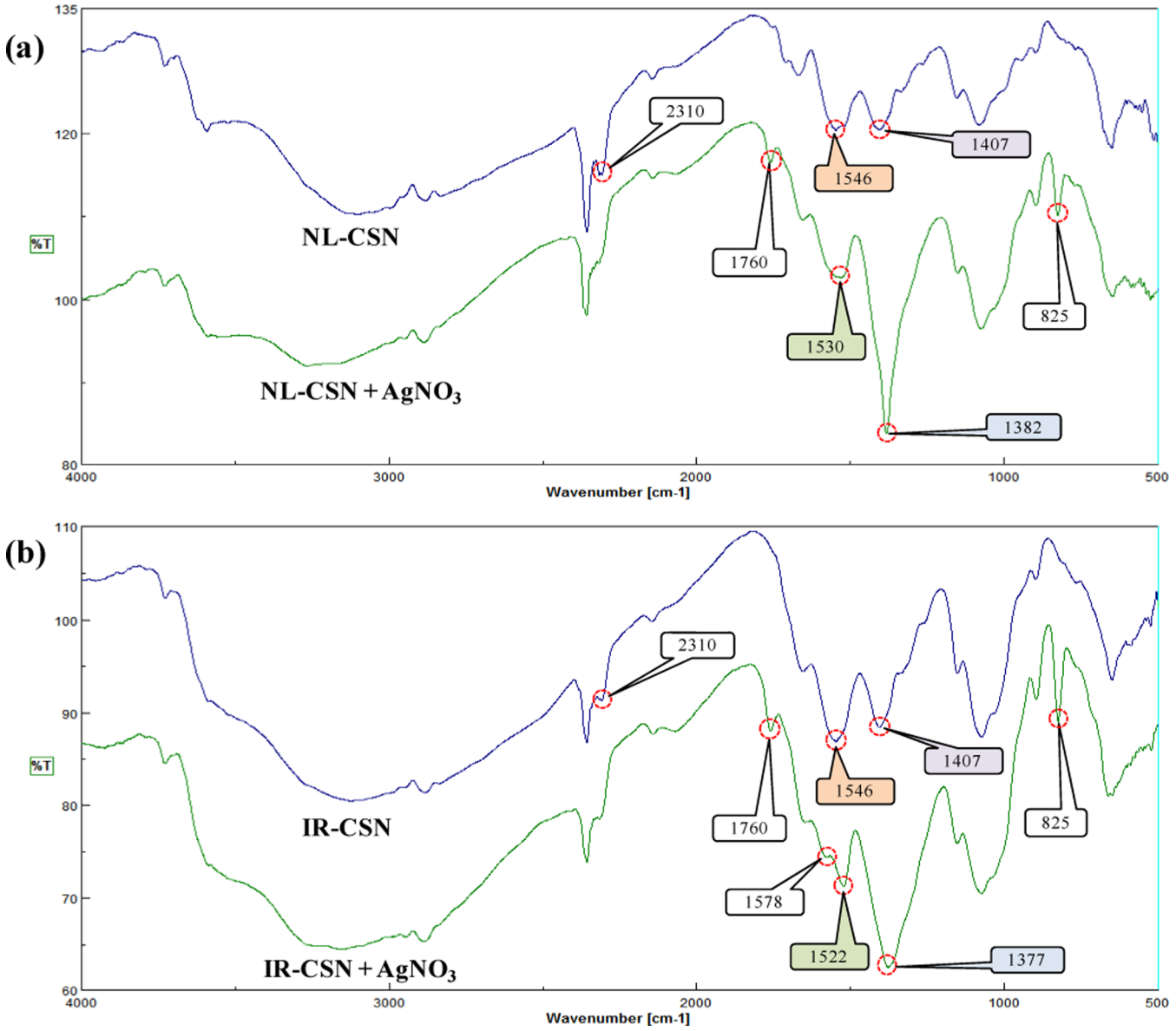

Figure 2. FTIR spectra of (a) NL-CSN and NL-CSN + $AgNO_3$ and (b) IR-CSN and IR-CSN + $AgNO_3$.

of the solution is a major indicator of the successful biosynthesis of noble metal nanoparticles. Concentration gradients of $AgNO_3$ and chitosans (NL-CSN and/or IR-CSN) showed a significant change in the color intensity after autoclave-assisted Ag NP synthesis. From visual observations, it was evident that the color intensity of the IR-CSN samples was very high compared to the NL-CSN samples (Figure 1a–d). The colorless 0.25% $AgNO_3$ solution turned light yellow to deep yellow with increasing concentration of NL-CSN (0–0.25%) (Figure 1a). In contrast, the colorless $AgNO_3$ (0.25%) solution turned light brown to dark brown and black with increasing concentration of IR-CSN (0–0.25%) (Figure 1c). However, the bare NL-CSN (0.25%) solution was colorless, whereas the 0.25% NL-CSN with 0.25% $AgNO_3$ had developed a deep-yellow color (Figure 1a,b). The intensity of this yellow color showed a gradual increase with increasing concentration of $AgNO_3$ (0–0.25%) (Figure 1b). In contrast, the bare IR-CSN (0.25%) solution had a light-brown color prior to addition of $AgNO_3$, and this brown color was attributed to the effect of γ-irradiation (100 kGy)-mediated polymer chain scission as reported earlier.[8−12] The intensity of the brown color further increased with an increase in the $AgNO_3$ concentration (0–0.25%) to form a deep-brown to black color (Figure 1d). The color changed with different concentrations of IR-CSN in $AgNO_3$ or vice versa, and this shows the direct correlation with the intensity of the absorbance (Figure 1c,d). In contrast, the absorbance spectra of NL-CSN + $AgNO_3$ (Figure 1a,b) were not clearly visible; rather, this showed a shallow elevation at the same dilution factor (100-fold) as of IR-CSN + $AgNO_3$. Such color change from yellow–pale yellow to brown–dark brown has been reported previously, confirming the formation of chitosan–Ag nanoparticles.[22,26−30]

2.2. UV–Visible Spectroscopy Study. Silver nanoparticles are known to display characteristic strong absorption peaks due to surface plasmon resonance (SPR). The presence of this SPR peak determined by UV–visible absorption spectra is a strong indication of the formation of silver nanoparticles. In the present study, the increasing concentration gradient (0–0.25%) of $AgNO_3$ with NL-CSN (0.25%) or vice versa did not

https://doi.org/10.1021/acsomega.1c05358
ACS Omega 2021, 6, 34812−34822

Scheme 1. Possible Scheme for Scissions of the Chitosan Polymer Due to γ-Irradiation (Based on Zainol et al.[9] and García et al.[10])

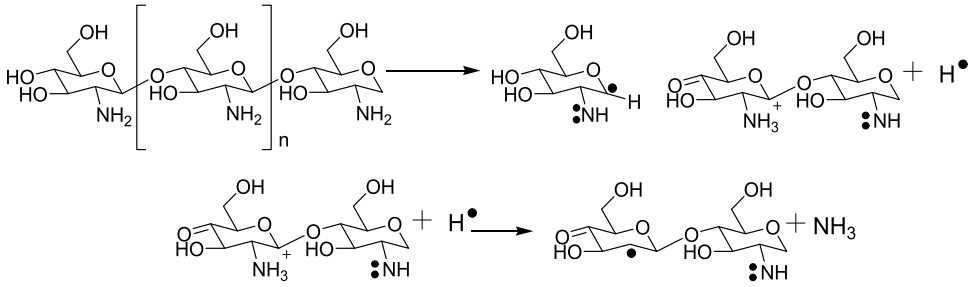

show noticeable SPR at a dilution factor of 100 (Figure 1a,b). On the other hand, the concentration gradient (0−0.25%) of $AgNO_3$ with IR-CSN (0.25%) or vice versa showed an intense SPR at 419−423 nm using the same dilution factor (Figure 1c,d). All of the UV−visible spectral observations exhibited the strongest absorption between 419 and 423 nm. Furthermore, with any concentration combination, there were no peaks around 335 and 560 nm, which confirmed the absence of nanoparticle aggregation.[31,32] The presence of this single strong SPR peak at around 420 nm corresponds to the typical SPR of conducting electrons from the surface of silver nanoparticles. The presence of similar SPR absorption has been reported at 410,[33] 420,[30,32] 424,[26] 425,[29] 426,[34] and 446 nm.[28] Increased SPR peak intensity corresponds to increased synthesis of Ag NPs, which is in turn due to an increase in the oxidation of hydroxyl groups of chitosan by silver ions.[31] In addition, Chen et al.[24] reported that reduction of silver using γ irradiation can be possible and found that an irradiation dose of 100 kGy was suitable to obtain evenly and densely dispersed silver nanoparticles. Lately, Affes et al. reported that Ag NPs synthesized using low-MW chitosan derivatives exhibited a maximum SPR absorption band with narrow spectra indicating the presence of less polydisperse nanoparticles.[22] In the present investigation, IR-CSN has been shown to have a higher potential to generate Ag NPs compared to NL-CSN, as IR-CSN is a degraded chitosan polymer as a result of γ-irradiation, which might have provided maximum access to silver ions to interact with hydroxyl groups of the polymer.

2.3. Fourier Transform Infrared (FTIR) Spectroscopy Study. FTIR-based characterization of chitosan polymers is advantageous as it can be implicated to determine the formation of new groups and cross-linking between chitosan molecules upon γ-irradiation.[35] From the FTIR spectra of NL-CSN and IR-CSN, with and without $AgNO_3$ (shown in Figure 2), it is evident that γ-irradiation did not result in major alterations, which corroborates with earlier reports.[11,12,14,35] γ Irradiation did not cause change in the polymer ring structure; rather, it resulted in the breakage of glycosidic bonds between chitosan monomers. An IR spectral band such as a band at 1546 cm^{-1} (that corresponds to $-NH_2$ bending of amide II), a band at 1407 cm^{-1} (that corresponds to OH bending vibrations of hydroxyl groups), and bands between 1074 and 1080 cm^{-1} (attributed to C−O and C−N stretching vibrations) were visible in both NL-CSN and IR-CSN. Based on these FTIR spectral band similarities between NL-CSN and IR-CSN, it was confirmed that upon γ irradiation there were no observable cross-linkings and alterations in the polymer ring structure. On the contrary, peculiar spectral variations were evident between chitosan and chitosan with $AgNO_3$ (Figure 2).

The spectral pattern was found to be very similar in NL-CSN and IR-CSN with $AgNO_3$. A prominent peak at 825 cm^{-1} was only evident in NL-CSN with $AgNO_3$ and IR-CSN with $AgNO_3$, which implicates the characteristic of C−H bending vibrations of stabilized silver nanoparticles, indicating that chitosan was involved in the process of stabilization.[30] There was a shift of the peak 1407 cm^{-1} of bare CSN (NL-CSN and/or IR-CSN) to 1382 cm^{-1} in NL-CSN + $AgNO_3$ and to 1377 cm^{-1} in IR-CSN + $AgNO_3$. A similar shift in the peak was also reported by Le et al. in the case of chitosan−Ag composites, which confirmed the coordination of $-NH_2$ groups of CSN with Ag^+/Ag^0 via electrostatic interactions.[36] Another shift of the peak 1546 cm^{-1} of bare CSN (NL-CSN and/or IR-CSN) to 1530 cm^{-1} in NL-CSN + $AgNO_3$ and to 1522 cm^{-1} in IR-CSN + $AgNO_3$ was observed (Figure 2). A similar shift in the $-NH_2$ group was also reported by Affes et al., as a result of the electrostatic interaction between $-NH_2$ groups of chitosan and Ag^+/Ag^0 leading to stabilization of Ag NPs.[22] Another peak at 2310 cm^{-1} was present in NL-CSN and IR-CSN, but it was absent in NL-CSN + $AgNO_3$ and IR-CSN + $AgNO_3$. Similar kinds of shifting of CSN peaks were also observed by Govindan et al.,[37] which was correlated with the interaction of Ag with CSN in the nanocomposite. An additional band at about 1578 cm^{-1} was present only in IR-CSN + $AgNO_3$, which corresponds to the N−H bending vibration. This band indicated the attachment of silver to nitrogen atoms, which increases the molecular weight and thereby reduces the vibration intensity of the N−H bond. Another new peak was present in both NL-CSN + $AgNO_3$ and IR-CSN + $AgNO_3$ at about 1760 cm^{-1} corresponding to carbonyl stretch vibrations in ketones, aldehydes, and carboxylic acids. The presence of this peak may indicate that the reduction of the silver ions is coupled to the oxidation of the hydroxyl groups in the chitosan molecule and/or its hydrolyzates.[38]

Irradiation induces a depolymerization reaction that causes the scission of the molecule, leading to shorter oligochitosan polymers through the chain scission mechanism (Scheme 1).[10] The scission occurs within the macromolecular structure of chitosan resulting in chain fragmentation. Furthermore, as scission does not result in alteration of functional groups, there were no changes in the FTIR spectra of all of the combinations, i.e., NL-CSN, IR-CSN, NL-CSN + $AgNO_3$, and IR-CSN + $AgNO_3$.

2.4. ζ Potential, Dynamic Light Scattering (DLS), and CHNS Analyses. ζ potential and DLS are deemed as vital parameters for the characterization of nanoparticles as well as for all colloidal systems. For NPs, ζ potential values can be positive or negative, which represents their stability in the given environment. At lower or neutral values of the ζ potential, the system is considered to be unstable and NPs

https://doi.org/10.1021/acsomega.1c05358
ACS Omega 2021, 6, 34812−34822

tend to cluster and precipitate. As a general consideration, ζ potential values larger than 20 (either positive or negative) favor stability of NPs in the liquid microenvironment.[39,40] In the present study, the ζ potential of bare chitosans (NL-CSN and IR-CSN) along with $AgNO_3$ showed values equal to 20 or above (Table 1). Similarly, Cinteza et al. reported positive ζ potential values, larger than 50−75 mV for chitosan-stabilized Ag NPs.[41] However, Long et al. reported positive ζ potentials of oligochitosan-stabilized silver nanoparticles synthesized by γ-irradiation, which were found stable over a wide range of pH.[23] Furthermore, the positive value is considered an advantage in the interaction of the particles with the negatively charged bacterial wall, leading to a better internalization.[41] However, negative ζ potentials of −27 and −21.4 mV were also reported to exhibit good stability.[29,30] The mean ζ potential of bare NL-CSN (+81.86 mV) was higher than that of bare IR-CSN (+44.57 mV), showing a correlation with the average molecular weights of both of the polymers (235 and 25 kDa, respectively) (Table 1). A similar trend in the reduction of ζ potentials proportional to a reduction in the MW of chitosan was reported wherein the ζ potential was higher when high-MW chitosan was used, while low-MW chitosan derivatives generated Ag NPs with the lowest ζ potentials.[22] However, in our case, after Ag nanoparticle synthesis, these ζ potential values further decreased for both NL-CSN + $AgNO_3$ (+44.43 mV) and IR-CSN + $AgNO_3$ (+19.66 mV) (Table 1).

Table 1. Variations in Physicochemical Characteristics of NL-CSN and IR-CSN and Formation of Ag Nanoparticles

sample	ζ potential (mV)	average particle size (nm)	PDI
NL-CSN (0.25%)	+81.86	1420.0	0.196
NL-CSN (0.25%) + $AgNO_3$ (0.25%)	+44.43	565.3	0.178
IR-CSN (0.25%)	+44.57	345.4	0.209
IR-CSN (0.25%) + $AgNO_3$ (0.25%)	+19.66	29.3	0.295

Chitosan has a high density of functional groups; therefore, it shows a very high ζ potential when added into the 1% solution of acetic acid, which is due to the formation of charged polyatomic molecules (shown in Scheme 2).[42] It is found that the ζ potential was decreased in the case of γ-irradiated chitosan, which might be due to the charged ions converting to the radicals after degradation.

There have been numerous reports on the formation of Ag NPs upon the γ-irradiation of $AgNO_3$ in water and other solutions. It has been observed that the Ag^+ ions are reduced by hydrated electrons e_{aq} produced during irradiation in solution.[43,44] The γ-irradiation-mediated reduction process can be written as follows

$$n{\cdot}H_2O \xrightarrow{\gamma\text{-rays}} e_{aq}^- + H^\bullet + OH^\bullet + H_3O + H_2 + \cdots$$

$$Ag^+ + e_{aq}^- \xrightarrow{\text{reduction}} Ag^0$$

As in the acetic water solution, the hydrogen atoms formed by hydrated electrons e_{aq} can also reduce the Ag^+ ions. Furthermore, the hydrogen radicals formed by the degradation of chitosan also help in reducing silver in Ag NPs. Chitosan acts as a stabilizing agent as well as a reducing agent. According to Modrzejewska et al., the −OH and $-NH_2$ groups in chitosan play a role in Ag^+ ion chelation.[45] The NH_2 groups of IR-CSN are well fixed with Ag atoms.[27] The more the polymer degradation, the more the interaction between Ag and the NH_2 group, and as a result, production of Ag NPs will be more.[24] In the present study, NL-CSN + $AgNO_3$ showed a yellowish color, indicating that a very small fraction of Ag NPs formed because only the chitosan has a role in the reduction of $AgNO_3$; there was no involvement of hydrated radicals in the absence of γ-irradiation. As the Ag^+ ions and the ions from chitosan reduced, the ζ potential was observed to be decreased in both of the cases of NL-CSN + $AgNO_3$ and IR-CSN + $AgNO_3$.

Dynamic light scattering (DLS) is considered a reliable and effective tool for assessment of particle size distribution of nanoscale materials dispersed in solution or colloidal suspensions.[46] From the DLS analysis of NL-CSN and IR-CSN, it was evident that the polymer particle size decreased drastically (from 1420 to 345.4 nm) due to γ-irradiation-mediated degradation (Table 1). This decrease directly correlates with the transmission electron microscopy (TEM) observation (Figure 3) although the values of average particle sizes were higher when measured using DLS. Such differences might be due to the effect of polymer capping and the

Scheme 2. Evidence-Based Prediction Scheme for Enhanced Formation of Ag Nanoparticles Due to Involvement of γ-Irradiated Chitosan (Modified after Nate et al.[42])

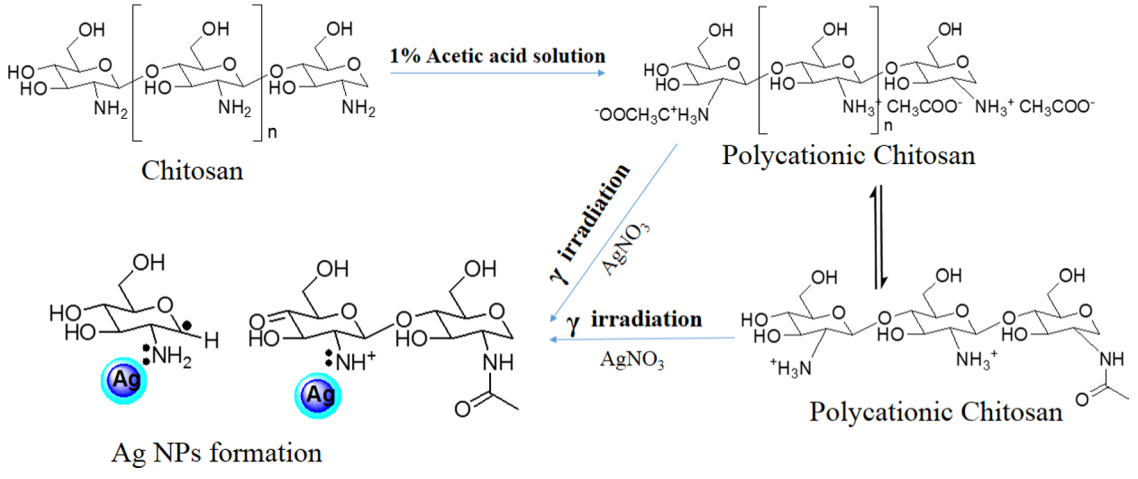

https://doi.org/10.1021/acsomega.1c05358
ACS Omega 2021, 6, 34812−34822

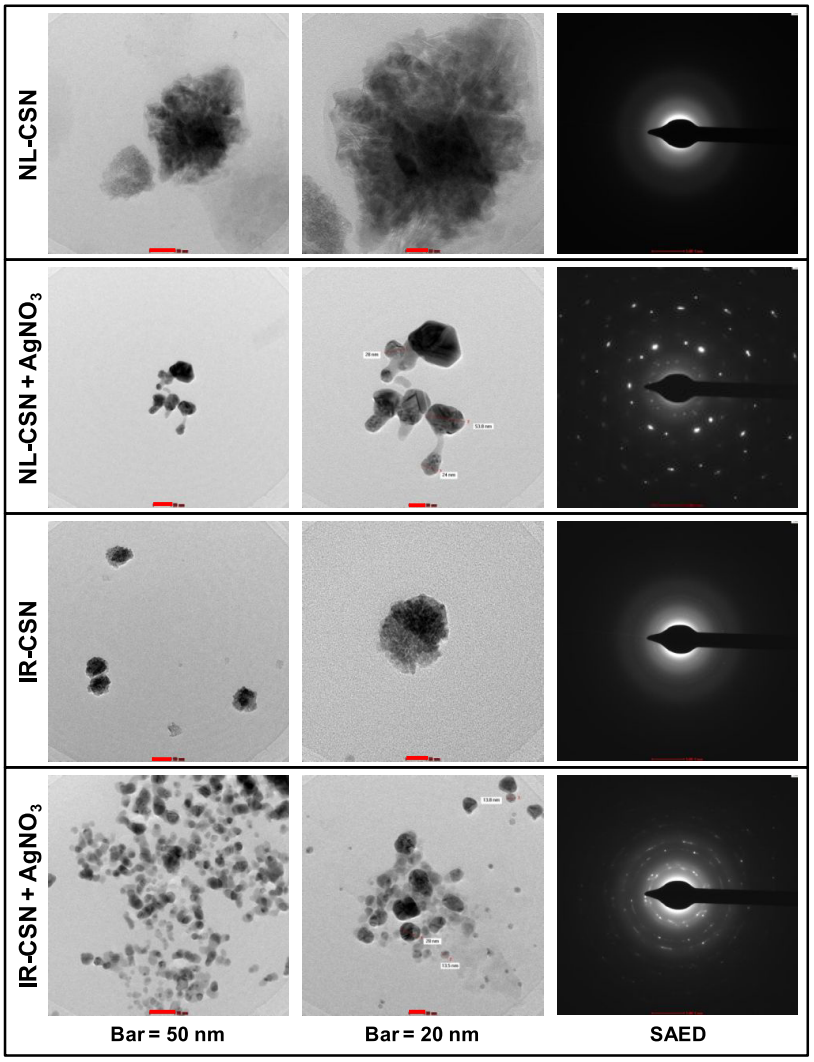

Figure 3. Transmission electron microscopy (TEM) images of NL-CSN, NL-CSN + $AgNO_3$, IR-CSN, and IR-CSN + $AgNO_3$.

influence of Brownian motion as reported earlier by Zhang et al.[47] and Affes et al.[22] Polydispersity index (PDI) values were at par for both of the polymers NL-CSN and IR-CSN; however, there was a noticeable difference found between NL-CSN + $AgNO_3$ and IR-CSN + $AgNO_3$ (Table 1). Formation of Ag nanoparticles with chitosans after autoclaving further decreased the particle size distribution. Results of ζ potential and average particle size have suggested that both ζ potential and particle size correlated with the MW of the polymer, and such a correlation was earlier reported by Affes et al.[22] Interestingly, the particle size was decreased by 2.5-fold in the case of NL-CSN (0.25%) + $AgNO_3$ (0.25%), while there was a sharp decrease (11.8-fold) in the case of IR-CSN (0.25%) + $AgNO_3$ (0.25%) (Table 1). This further confirmed that synthesis of Ag NPs was more in the case of IR-CSN than that of NL-CSN.

Elemental (CHNS) analysis was performed to determine the relative changes in elemental content that would occur after interaction with $AgNO_3$. From the CHNS-based elemental analysis, it was evident that there were no changes in carbon, hydrogen, and nitrogen contents in the cases of bare NL-CSN (0.25%) and bare IR-CSN (0.25%) (Table 2). This infers that after γ-irradiation-mediated degradation, the radicals and the amine group remained in the same solutions and there were no other changes in terms of additions, removal, or substitutions. However, significant changes in the C, H, and N contents were observed in the sample containing $AgNO_3$ (0.25%); this confirmed the binding of Ag with the chitosan molecule. Furthermore, IR-CSN + $AgNO_3$ had a lower C/N ratio than NL-CSN + $AgNO_3$ (Table 2). In contrast, an increased C/N ratio was reported for chitosan−silica composites compared to chitosan.[48]

Table 2. Variations in the CHNS Content of NL-CSN and IR-CSN upon γ-Irradiation and after Synthesis of Ag Nanoparticles[a]

	average CHNS content (%)				
sample	C	H	N	S	C/N ratio[a]
bare NL-CSN (0.25%)	36.8	7.1	5.6	0.0	6.6
NL-CSN (0.25%) + $AgNO_3$ (0.25%)	20.7	4.2	7.0	0.0	3.0
bare IR-CSN (0.25%)	37.2	7.1	5.5	0.0	6.8
IR-CSN (0.25%) + $AgNO_3$ (0.25%)	19.9	3.8	7.3	0.0	2.7

[a]C/N ratio, carbon/nitrogen ratio.

2.5. Transmission Electron Microscopy (TEM). Morphological peculiarity and particle size of the synthesized Ag

https://doi.org/10.1021/acsomega.1c05358
ACS Omega 2021, 6, 34812−34822

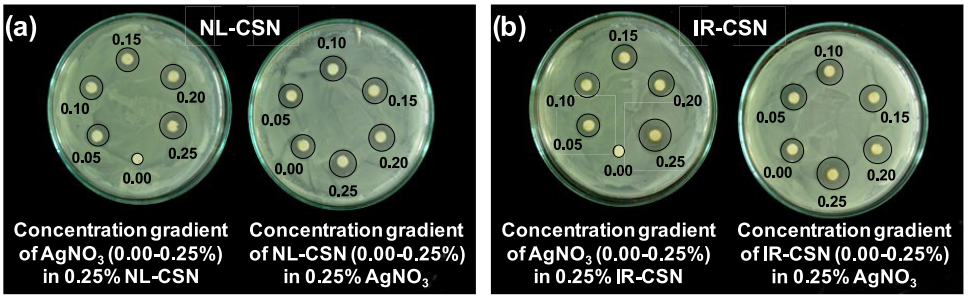

Figure 4. Antibacterial activity (against *E. coli*) of (a) NL-CSN and (b) IR-CSN with different concentration gradients of $AgNO_3$.

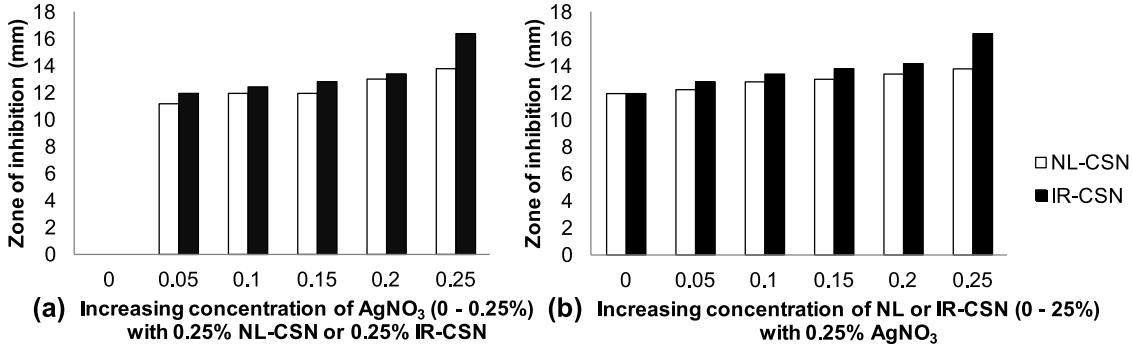

Figure 5. Antimicrobial activity of different concentration gradients of NL-CSN (0−0.25%) and IR-CSN (0−0.25%) with $AgNO_3$ (0−0.25%). (a) Effect of increasing concentration of $AgNO_3$ along with NL-CSN (0.25%) and IR-CSN (0.25%). (b) Effect of increasing concentration of NL-CSN and IR-CSN along with $AgNO_3$ (0.25%).

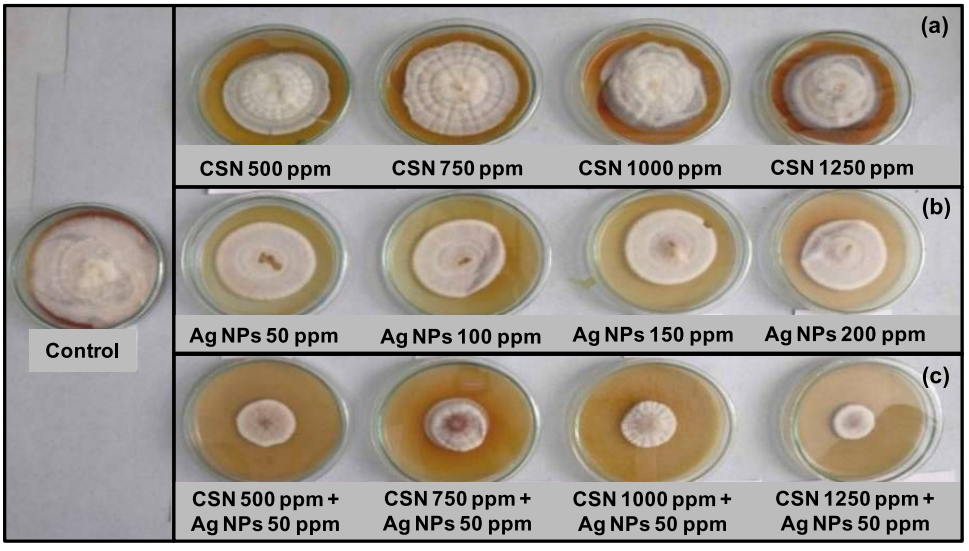

Figure 6. Antifungal activity (against *F. oxysporum* f. sp. *ciceris*) of (a) IR-CSN alone at different concentrations, (b) Ag NPs alone at different concentrations, and (c) combination of Ag NPs at 50 ppm + different concentrations of IR-CSN.

NPs were investigated by TEM analysis, and micrographs at different magnifications are shown in Figure 3. The decrease in cluster size of the chitosan polymer was found after the γ-irradiation in IR-CSN. γ-Irradiation has two major effects on the chitosan polymer. First, the energy transfer due to irradiation could induce fragmentations of covalent bonds in the chitosan and produce the free radicals.[35] Irradiation induces the depolymerization reaction that causes the scission of the molecule, leading to smaller chitosan chains. This was also observed from DLS analysis that after the irradiation the size of NL-CSN decreased from 1420 to 345.4 nm in IR-CSN (Table 1). Furthermore, the metallic nature of Ag nanoparticles was confirmed by selected area electron diffraction (SAED) (Figure 3).

The patterns of concentric diffraction rings corresponding to the different crystallographic planes of metallic silver suggested the synthesis of polycrystalline silver nanoparticles. However, SAED patterns of bare NL-CSN and bare IR-CSN samples confirmed their noncrystalline nature. A significant difference in the morphology and SAED pattern was observed between NL-CSN + $AgNO_3$ and IR-CSN + $AgNO_3$. This indicated the formation of silver nanoparticles in the polymeric lattice of the chitosan and was more in the case of IR-CSN + $AgNO_3$ (Figure 3). Based on the TEM images, the size of Ag NPs was

https://doi.org/10.1021/acsomega.1c05358
ACS Omega 2021, 6, 34812−34822

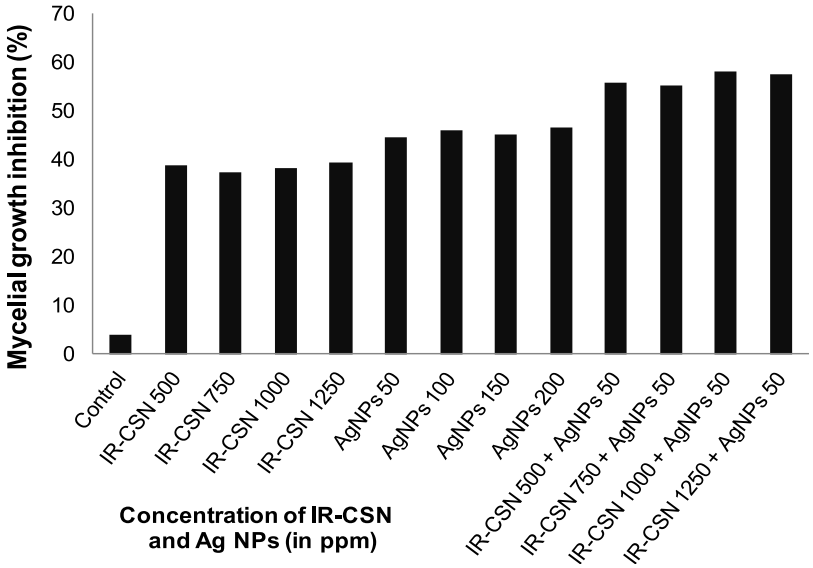

Figure 7. Effect of IR-CSN, Ag NPs, and IR-CSN + Ag NPs on mycelia growth of *F. oxysporum* f. sp. *ciceris*.

found to be between 24 and 55 nm in the case of NL-CSN + $AgNO_3$, whereas it was between 13 and 32 nm in the case of IR-CSN + $AgNO_3$. This indicated that the particle size distribution was narrow for IR-CSN + $AgNO_3$ compared to NL-CSN + $AgNO_3$. A similar kind of influence of chitosan polymer characteristics, particularly its MW, on the morphology of silver nanoparticles has been reported earlier.[22]

2.6. Assessment of Antimicrobial Activity of CSN−Ag Nanocomposites. Synthesis of Ag NPs was attempted in different combinations of NL-CSN (0−0.25%) in $AgNO_3$ (0−0.25%) and IR-CSN (0−0.25%) in $AgNO_3$ (0−0.25%) and vice versa. The antibacterial assay performed against *E. coli* showed differences in the inhibition of bacterial growth (Figures 4 and 5).

In the case of chitosan (either NL-CSN or IR-CSN) with a concentration gradient of $AgNO_3$ (0−0.25%), the antimicrobial activity increased with increasing $AgNO_3$ concentration. Neither NL-CSN nor IR-CSN showed any inhibition zone at 0.25% concentration. However, $AgNO_3$ alone showed an inhibition zone (12 mm), which might be as a result of toxicity of Ag ions at 0.25% $AgNO_3$. Among the different combinations of NL-CSN, maximum inhibition (13.8 mm) was recorded at 0.25% NL-CSN + 0.25% $AgNO_3$. On the other hand, it was clearly evident that of all of the combinations of IR-CSN, the highest antibacterial activity (16.4 mm) was recorded at 0.25% IR-CSN + 0.25% $AgNO_3$, suggesting that IR-CSN + $AgNO_3$ had the maximum antimicrobial property compared to that of NL-CSN + $AgNO_3$. A similar antibacterial activity of chitosan−silver nanoparticles against *E. coli* was previously reported by Venkatesham et al.,[31] Kalaivani et al.,[26] Akmaz et al.,[49] and Chen et al.[50]

The antifungal activity of IR-CSN + $AgNO_3$ was evaluated against chickpea wilt pathogen *Fusarium oxysporum* f. sp. *ciceris*. Out of different concentration combinations of IR-CSN (500, 750, 1000, 1250 ppm) tested, 1250 ppm showed the maximum inhibitory effect (Figure 6). On the other hand, out of different concentrations of Ag NPs (50, 100, 150, 200 ppm), Ag NPs at 50 ppm were found to have the maximum inhibition of mycelial growth (Figure 7). However, IR-CSN (500, 750, 1000, 1250 ppm) when used in combination with Ag NPs (50 ppm) showed an additive synergistic activity when compared to that of Ag NPs alone. Similar results were reported earlier wherein chitosan−copper oxide (Ch−CuO) nanocomposites and chitosan−zinc oxide (Ch−ZnO) nanocomposites were found to be effective against *F. oxysporum* f. sp. *ciceri*.[51] Antifungal activities of chitosan nanoparticles and chitosan−silver nanocomposites were also reported against the *F. oxysporum* species complex causing infection in zebrafish.[52]

In our earlier studies, we evaluated enhanced biological properties of IR-CSN in alleviation of biotic stresses in different crop plants such as in onion against *Alternaria porri*,[16] in pea against powdery mildew,[15] as well as abiotic stresses in potato[12] and sugarcane.[14] Lately, the chitosan−silver nanocomposite along with *Trichoderma viridae* was found to impart a synergistic effect against *Ceratocystis paradoxa* (which causes pineapple disease of sugarcane).[53] With the same perspective, in the present study, we evaluated the differential potential of high-MW NL-CSN and γ-irradiated low MW IR-CSN for enhanced chitosan−Ag NP synthesis. γ-Irradiated chitosan (IR-CSN) was found to mediate the enhanced synthesis of Ag nanocomposites bearing superior physicochemical and biological properties than that of NL-CSN. In our earlier studies, γ-irradiated chitosan (IR-CSN) was characterized to have enhanced biological properties and, in this study, IR-CSN has been further utilized for Ag NP synthesis resulting in synergistic effects against important phytopathogenic fungi such as *F. oxysporum*.

3. CONCLUSIONS

In the present study, our results showed that γ-irradiated low-MW chitosan (IR-CSN) had a higher efficiency of Ag reduction and stabilization compared to high-MW NL-CSN. Different physicochemical analyses clearly showed that γ irradiation could cleave the long chitosan polymer, which enabled the interaction of the Ag ion at a higher frequency resulting in more reduction of silver to form Ag nanoparticles. Furthermore, FTIR, DLS, ζ potential, and elemental (CHNS) analyses confirmed the formation of stable nanocomposites. The antimicrobial activity of chitosan−Ag nanocomposites was found to have potential synergistic antifungal activity against *F. oxysporum*. The γ-irradiated chitosan-mediated enhanced Ag nanoparticle synthesis could be further explored to develop

https://doi.org/10.1021/acsomega.1c05358
ACS Omega 2021, 6, 34812−34822

biogenic, chitosan-based nanoformulations to be used as antibacterial and antifungal control agents against phytopathogenic organisms in sustainable agriculture.

4. MATERIALS AND METHODS

4.1. Materials. Chitosan (NL-CSN) from shrimp shells having a high molecular weight (MW) (~235 kDa) and 85% degree of deacetylation was used. Silver nitrate ($AgNO_3$) and glacial acetic acid were from SD Fine Chem; Luria−Bertani (LB) broth and LB agar media were from HiMedia Chemicals. Analytical-grade chemicals were used without any further purification.

4.2. Chitosan Polymer Preparation and Degradation. γ-Irradiated chitosan (IR-CSN) with low MW (25 kDa) was prepared as described previously by Mirajkar et al.[14] Briefly, a chitosan solution (2% w/v) was prepared by slowly dispersing chitosan powder in 1% (v/v) glacial acetic acid prepared in double-distilled water. The mixture was agitated using a high-speed vortex mixer to disperse the aggregates and allowed to stand overnight. This clear viscous solution was then packaged in polybags of appropriate dimensions and exposed to γ radiation (100 kGy) using a cobalt-60 (^{60}C) γ irradiator (at dose rate 2.1 kGy/h) at the Food Technology Division, Bhabha Atomic Research Centre, Trombay, Mumbai, India.

4.3. Concentration Gradient of Chitosan and $AgNO_3$ for Synthesis of Chitosan−Silver Nanocomposites. Chitosan−silver nanoparticles (CSN−Ag NPs) were synthesized using the green synthesis method as described by Venkatesham et al. with a few modifications.[31] Normal (NL-CSN) and γ-irradiated chitosan (IR-CSN) solutions (2% w/v) were diluted to 0.5% (w/v) working concentration in distilled water. The $AgNO_3$ solution (0.5% w/v) was freshly prepared in double-distilled water. To study the effect of concentration of chitosan on Ag nanoparticle synthesis, the concentration gradient of chitosans (0−0.25%) was made in 0.25% $AgNO_3$. Similar to the study effect of $AgNO_3$ concentration on Ag nanoparticle synthesis, the concentration gradient of $AgNO_3$ (0−0.25%) was made in 0.25% chitosan. These concentration gradients were prepared for both types of chitosans, NL-CSN and IR-CSN (Table S1). Chitosan solution (0.5%) was mixed with an appropriate volume of $AgNO_3$ to obtain the concentration gradient (0−0.5%) and vice versa. Absolute control solutions were kept for each combination. All tubes were placed in an autoclave (NAT Steel, Mumbai) for 20 min at 121 °C and 15 psi pressure. Tubes were then allowed to cool to room temperature.

4.4. Characterization of Chitosan−Silver Nanocomposites. All concentration gradient combinations were analyzed by UV−visible spectroscopy and antimicrobial activity. However, both the respective absolute bare chitosans (NL-CSN and IR-CSN at 0.25%) and chitosans with 0.25% NL-CSN + 0.25% $AgNO_3$ and 0.25% IR-CSN + 0.25% $AgNO_3$ were selected for the rest of the other characterization methods, i.e., FTIR, ζ potential, CHNS elemental analysis, TEM, etc.

4.4.1. UV−Visible and Fourier Transform Infrared (FTIR) Spectroscopy. UV−visible spectra (200−800 nm) were recorded on a double-beam spectrophotometer (Perkin) using quartz cuvettes of 10 mm path length. For this, an aliquot of each concentration gradient was diluted 100 times (i.e., 10 μL of nanocomposite in 990 μL of deionized water). For FTIR spectroscopy, pellets of vacuum-dried sample aliquots were prepared in an agate mortar by mixing with dry KBr (in a 1:50 proportion). FTIR spectral measurements were carried out using an FTIR spectrometer (Jasco FT-IR 660 Plus) in the spectral range frequencies of 500−4000 cm^{-1} at room temperature (25 °C).

4.4.2. ζ Potential, DLS, and Elemental (CHNS) Measurements. Appropriate volumes of aliquots were analyzed for ζ potential and particle size using a zetasizer and DLS, respectively (Brookhaven Instruments). ζ potential was carried out at an effective voltage of 150 V and 25 °C triplicate. The sample properties were further analyzed by elemental content, CHNS, using the Analyzer Vario Micro Cube (Elementer, Germany).

4.4.3. Transmission Electron Microscopic (TEM) Analysis. Sample grids for TEM imaging were prepared by placing a drop of chitosan−Ag nanocomposite suspension onto a carbon-coated copper grid and allowed to dry in a laboratory hood at room temperature. TEM micrographs and selected area electron diffraction (SAED) data were acquired using Philips CM-200 and FEI model G2 microscopes.

4.5. Assessment of Antimicrobial Activity. The antimicrobial activity of each concentration gradient was evaluated against *E. coli* by the disc diffusion assay. An overnight-grown *E. coli* culture in a Luria−Bertani (LB) broth medium was used to make spread plates on the LB agar medium. Aliquots of test suspensions (20 μL) were carefully loaded on sterile paper discs (5 mm diameter) placed on LB agar plates. Plates were incubated in an incubator at 37 °C, and then, the diameter (mm) of the zone of inhibition was observed after 24 h. Furthermore, the antifungal activity was assessed against chickpea wilt pathogen by evaluation of mycelial growth inhibition. A pure culture of *F. oxysporum* f. sp. *ciceris* was obtained from the Plant Pathology Section of Vasantdada Sugar Institute, Manjari, Pune. Fresh mycelial discs were taken from the pure culture and were inoculated on a potato dextrose agar (PDA) medium supplemented with different concentrations of Ag NPs (0, 50, 100, 150, 200 ppm). Alongside, PDAs supplemented with IR-CSN at different concentrations (0, 500, 650, 1000, 1250 ppm) were used as controls to assess the effect of IR-CSN on mycelia growth. In addition, combination of Ag NPs with IR-CSN was used to evaluate synergistic effects of Ag NPs (50 ppm) with different concentrations of IR-CSN (0, 500, 650, 1000, 1250 ppm). The radial diameter of mycelium was recorded after 9 days of incubation at 28 °C.

■ ASSOCIATED CONTENT

Supporting Information

The Supporting Information is available free of charge at https://pubs.acs.org/doi/10.1021/acsomega.1c05358.

Concentration gradient used for the synthesis of chitosan−silver nanocomposites (Table S1) (PDF)

■ AUTHOR INFORMATION

Corresponding Author

Sunil Dalvi − *Plant Tissue Culture Section, Vasantdada Sugar Institute, Pune 412307, India*; Email: sgdalvi@gmail.com, sg.dalvi@vsisugar.org.in

Authors

Shriram Mirajkar − *Plant Tissue Culture Section, Vasantdada Sugar Institute, Pune 412307, India*; Present Address: School of Nanoscience and Biotechnology,

https://doi.org/10.1021/acsomega.1c05358
ACS Omega 2021, 6, 34812−34822

Shivaji University, Kolhapur 416004, India; orcid.org/0000-0002-4513-1536

Prakash Rathod − *Department of Chemistry, Savitribai Phule Pune University, Pune 411007, India;* Present Address: Department of Chemistry, Shri Sadguru Saibaba Science and Commerce College, Ashti, Gadchiroli 442707, India

Bharat Pawar − *Plant Pathology Section, Vasantdada Sugar Institute, Pune 412307, India*

[⊥]**Suprasanna Penna** − *Nuclear Agriculture and Biotechnology Division, Bhabha Atomic Research Centre, Mumbai 400085, India;* orcid.org/0000-0002-6572-6190

Complete contact information is available at: https://pubs.acs.org/10.1021/acsomega.1c05358

Author Contributions

S.M., S.D., B.P., and S.P. conceived, planned, and executed the experiments. P.R. provided expertise in characterization methods. S.M., P.R., B.P., S.D., and S.P. analyzed the data and wrote the manuscript.

Notes

The authors declare no competing financial interest.

[⊥]Former scientist.

■ ACKNOWLEDGMENTS

The authors are thankful to the Director General, Vasantdada Sugar Institute, Manjari (Bk.), Pune, India, for providing necessary facilities. The authors are thankful to Dr. Jitendra Kumar, BARC, Mumbai for providing the FTIR spectroscopy facility for the present study.

■ REFERENCES

(1) Orzali, L.; Corsi, B.; Forni, C.; Riccioni, L. Chitosan in Agriculture: A New Challenge for Managing Plant Disease. In *Biological Activities and Application of Marine Polysaccharides*; Shalaby, E., Ed.; InTech: Rijeka, 2017.

(2) Aranaz, I.; Acosta, N.; Civera, C.; Elorza, B.; Mingo, J.; Castro, C.; Gandia, M. L.; Heras, A. C. Cosmetics and cosmeceutical applications of chitin, chitosan and their derivatives. *Polymers* **2018**, *10*, No. 213.

(3) Morin-Crini, N.; Lichtfouse, E.; Torri, G.; Crini, G. Applications of chitosan in food, pharmaceuticals, medicine, cosmetics, agriculture, textiles, pulp and paper, biotechnology, and environmental chemistry. *Environ. Chem. Lett.* **2019**, *17*, 1667−1692.

(4) Malerba, M.; Cerana, R. Chitosan effects on plant systems. *Int. J. Mol. Sci.* **2016**, *17*, No. 996.

(5) Wattjes, J.; Sreekumar, S.; Richter, C.; Cord-Landwehr, S.; Singh, R.; El Gueddari, N. E.; Moerschbacher, B. M. Patterns matter part 1: Chitosan polymers with non-random patterns of acetylation. *React. Funct. Polym.* **2020**, *151*, No. 104583.

(6) Li, J.; Zhuang, S. Antibacterial activity of chitosan and its derivatives and their interaction mechanism with bacteria: Current state and perspectives. *Eur. Polym. J.* **2020**, *138*, No. 109984.

(7) El Hadrami, A.; Adam, L. R.; El Hadrami, I.; Daayf, F. Chitosan in plant protection. *Mar. Drugs* **2010**, *8*, 968−987.

(8) Choi, W. S.; Ahn, K. J.; Lee, D. W.; Byun, M. W.; Park, H. J. Preparation of chitosan oligomers by irradiation. *Polym. Degrad. Stab.* **2002**, *78*, 533−538.

(9) Zainol, I.; Akil, H. M.; Mastor, A. Effect of γ-irradiation on the physical and mechanical properties of chitosan powder. *Mater. Sci. Eng., C* **2009**, *29*, 292−297.

(10) García, M. A.; de la Paz, N.; Castro, C.; Rodríguez, J. L.; Rapado, M.; Zuluaga, R.; Ganan, P.; Casariego, A. Effect of molecular weight reduction by gamma irradiation on the antioxidant capacity of chitosan from lobster shells. *J. Radiat. Res. Appl. Sci.* **2015**, *8*, 190−200.

(11) Muley, A. B.; Ladole, M. R.; Suprasanna, P.; Dalvi, S. G. Intensification in biological properties of chitosan after γ-irradiation. *Int. J. Biol. Macromol.* **2019**, *131*, 435−444.

(12) Muley, A. B.; Shingote, P. R.; Patil, A. P.; Dalvi, S. G.; Suprasanna, P. Gamma radiation degradation of chitosan for application in growth promotion and induction of stress tolerance in potato (*Solanum tuberosum* L.). *Carbohydr. Polym.* **2019**, *210*, 289−301.

(13) Dalvi, S. G.; Waghey, P.; Pawar, B. H.; Suprasanna, P. *In vitro* study on the antifungal effects of chitosan and oligochitosan on early blight disease in potato. *J. Chitin Chitosan Sci.* **2015**, *3*, 46−52.

(14) Mirajkar, S. J.; Dalvi, S. G.; Ramteke, S. D.; Suprasanna, P. Foliar application of gamma radiation processed chitosan triggered distinctive biological responses in sugarcane under water deficit stress conditions. *Int. J. Biol. Macromol.* **2019**, *139*, 1212−1223.

(15) Kamble, P. K.; Lohate, S. R.; Hasabnis, S. N.; Dalvi, S. G.; Choudhari, S. R. Efficacy of GI Chitosan in management of powdery mildew of pea. *Int. J. Curr. Microbiol. Appl. Sci.* **2019**, *8*, 1879−1885.

(16) Gaikwad, H. D.; Hasabnis, S. N.; Dalvi, S. G. Oligochitosan as an effective modulator to manage the yield and productivity of onion infected by *Alternaria porri*. *Int. J. Curr. Microbiol. Appl. Sci.* **2019**, *8*, 555−561.

(17) Siddiqi, K. S.; Husen, A.; Rao, R. A. K. A review on biosynthesis of silver nanoparticles and their biocidal properties. *J. Nanobiotechnol.* **2018**, *16*, No. 14.

(18) Mehmood, A. Brief overview of the application of silver nanoparticles to improve growth of crop plants. *IET Nanobiotechnol.* **2018**, *12*, 701−705.

(19) Sreeprasard, T. S.; Pradeep, T. Noble Metal Nanoparticles. In *Springer Handbook of Nanomaterials*; Vajtai, R., Ed.; Springer: Berlin, Heidelberg, 2013; pp 303−388.

(20) Pirtarighat, S.; Ghannadnia, M.; Baghshahi, S. Green synthesis of silver nanoparticles using the plant extract of *Salvia spinosa* grown *in vitro* and their antibacterial activity assessment. *J. Nanostruct. Chem.* **2019**, *9*, 1−9.

(21) Yu, J.; Wang, D.; Geetha, N.; Khawar, K. M.; Jogaiah, S.; Mujtaba, M. Current trends and challenges in the synthesis and applications of chitosan-based nanocomposites for plants: A review. *Carbohydr. Polym.* **2021**, *261*, No. 117904.

(22) Affes, S.; Maalej, H.; Aranaz, I.; Kchaou, H.; Acosta, N.; Heras, A.; Nasri, M. Controlled size green synthesis of bioactive silver nanoparticles assisted by chitosan and its derivatives and their application in biofilm preparation. *Carbohydr. Polym.* **2020**, *236*, No. 116063.

(23) Long, D.; Wu, G.; Chen, S. Preparation of oligochitosan stabilized silver nanoparticles by gamma irradiation. *Radiat. Phys. Chem.* **2007**, *76*, 1126−1131.

(24) Chen, P.; Song, L.; Liu, Y.; Fang, Y. Synthesis of silver nanoparticles by γ-ray irradiation in acetic water solution containing chitosan. *Radiat. Phys. Chem.* **2007**, *76*, 1165−1168.

(25) Phu, D. V.; Lang, V. T. K.; Lan, N. T. K.; Duy, N. N.; Chau, N. D.; Du, B. D.; Cam, B. D.; Hien, N. Q. Synthesis and antimicrobial effects of colloidal silver nanoparticles in chitosan by γ-irradiation. *J. Exp. Nanosci.* **2010**, *5*, 169−179.

(26) Kalaivani, R.; Maruthupandy, M.; Muneeswaran, T.; Hameedha Beevi, A.; Anand, M.; Ramakritinan, C. M.; Kumaraguru, A. K. Synthesis of chitosan mediated silver nanoparticles (Ag NPs) for potential antimicrobial applications. *Front. Lab. Med.* **2018**, *2*, 30−35.

(27) Susilowati, E.; Maryani; Ashadi. Green synthesis of silver-chitosan nanocomposite and their application as antibacterial material. *J. Phys.: Conf. Ser.* **2019**, *1153*, No. 012135.

(28) Alshehri, M. A.; Aziz, A. T.; Trivedi, S.; Panneerselvam, C. Efficacy of chitosan silver nanoparticles from shrimp-shell wastes against major mosquito vectors of public health importance. *Green Process. Synth.* **2020**, *9*, 675−684.

(29) Rezazadeh, N. H.; Buazar, F.; Matroodi, S. Synergistic effects of combinatorial chitosan and polyphenols biomolecules on enhanced

antibacterial activity of biofunctionalized silver nanoparticles. *Sci. Rep.* **2020**, *10*, No. 19615.
(30) Parthasarathy, A.; Vijayakumar, S.; Malaikozhundan, B.; Thangaraj, M. P.; Ekambaram, P.; Murugan, T.; Velusamy, P.; Anbu, P.; Vaseeharan, B. Chitosan-coated silver nanoparticles promoted antibacterial, antibiofilm, wound-healing of murine macrophages and antiproliferation of human breast cancer MCF 7 cells. *Polym. Test.* **2020**, *90*, No. 106675.
(31) Venkatesham, M.; Ayodhya, D.; Madhusudhan, A.; Veera Babu, N.; Veerabhadram, G. A novel green one-step synthesis of silver nanoparticles using chitosan: catalytic activity and antimicrobial studies. *Appl. Nanosci.* **2014**, *4*, 113−119.
(32) Zhou, Y.; Zhao, Y.; Wang, L.; Xu, L.; Zhai, M.; Wei, S. Radiation synthesis and characterization of nanosilver/gelatin/carboxymethyl chitosan hydrogel. *Radiat. Phys. Chem.* **2012**, *81*, 553−560.
(33) Sanpui, P.; Murugadoss, A.; Prasad, P. V.; Ghosh, S. S.; Chattopadhyay, A. The antibacterial properties of a novel chitosan-Ag-nanoparticle composite. *Int. J. Food Microbiol.* **2008**, *124*, 142−146.
(34) Murugan, K.; Anitha, J.; Suresh, U.; Rajaganesh, R.; Panneerselvam, C.; Aziz, A. T.; Tseng, L. C.; Kalimuthu, K.; Alsalhi, M. S.; Devanesan, S.; Nicoletti, M.; Sarkar, S. K.; Benelli, G.; Hwang, J. S. Chitosan-fabricated Ag nanoparticles and larvivorous fishes: A novel route to control the coastal malaria vector Anopheles sundaicus? *Hydrobiologia* **2017**, *797*, 335−350.
(35) Desai, K. G.; Park, H. J. Study of gamma-irradiation effects on chitosan microparticles. *Drug Delivery* **2006**, *13*, 39−50.
(36) Le, V. T.; Bach, L. G.; Pham, T. T.; Le, N. T. T.; Ngoc, U. T. P.; Tran, D. H. N.; Nguyen, D. H. Synthesis and antifungal activity of chitosan-silver nanocomposite synergize fungicide against *Phytophthora capsici*. *J. Macromol. Sci., Part A: Pure Appl. Chem.* **2019**, 522−528.
(37) Govindan, S.; Nivethaa, E. A. K.; Saravanan, R.; Narayanan, V.; Stephen, A. Synthesis and characterization of chitosan−silver nanocomposite. *Appl. Nanosci.* **2012**, *2*, 299−303.
(38) Wei, D.; Sun, W.; Qian, W.; Ye, Y.; Ma, X. The synthesis of chitosan-based silver nanoparticles and their antibacterial activity. *Carbohydr. Res.* **2009**, *344*, 2375−2382.
(39) Honary, S.; Brabadi, H.; Gharaei-Fathabada, E.; Naghibi, F. Green synthesis of copper oxide nanoparticles using *Penicillium aurantiogriseum*, *Penicillium citrinum* and *Penicillium waksmani*. *Dig. J. Nanomater. Biostruct.* **2012**, *7*, 999−1005.
(40) Moraru, C.; Mincea, M.; Menghiu, G.; Ostafe, V. Understanding the factors influencing chitosan-based nanoparticles-protein corona interaction and drug delivery applications. *Molecules* **2020**, *25*, No. 4758.
(41) Cinteza, L. O.; Scomoroscenco, C.; Voicu, S. N.; Nistor, C. L.; Nitu, S. G.; Trica, B.; Jecu, M. L.; Petcu, C. Chitosan-stabilized Ag nanoparticles with superior biocompatibility and their synergistic antibacterial effect in mixtures with essential oils. *Nanomaterials* **2018**, *8*, No. 826.
(42) Nate, Z.; Moloto, M. J.; Mubiayi, P. K.; Sibiya, P. N. Green synthesis of chitosan capped silver nanoparticles and their antimicrobial activity. *MRS Adv.* **2018**, *3*, 2505−2517.
(43) Zhu, Y. J.; Qian, Y.; Li, X.; Zhang, M. γ-radiation synthesis and characterization of polyacrylamide−silver nanocomposites. *Chem. Commun.* **1997**, *12*, 1081−1082.
(44) Bogle, K. A.; Dhole, S. D.; Bhoraskar, V. N. Silver nanoparticle: synthesis and size control by electron irradiation. *Nanotechnology* **2006**, *17*, 3204−3208.
(45) Modrzejewska, Z.; Dorabialska, M.; Zarzycki, R.; Wojtasz-Pająk, A. The Mechanism of Sorption of Ag^{+} Ions on Chitosan Microgranules: IR and NMR Studies. *Progress on Chemistry and Application of Chitin and its Derivatives*; Polskie Towarzystwo Chitynowe, 2009; Vol *14*, pp 49−64.
(46) Sapsford, K. E.; Tyner, K. M.; Dair, B. J.; Deschamps, J. R.; Medintz, I. L. Analyzing nanomaterial bioconjugates: a review of current and emerging purification and characterization techniques. *Anal. Chem.* **2011**, *83*, 4453−4488.
(47) Zhang, X. F.; Liu, Z. G.; Shen, W.; Gurunathan, S. Silver nanoparticles: Synthesis, characterization, properties, applications, and therapeutic approaches. *Int. J. Mol. Sci.* **2016**, *17*, No. 1534.
(48) Budnyak, T. M.; Pylypchuk, I. V.; Tertykh, V. A.; Yanovska, E. S.; Kolodynska, D. Synthesis and adsorption properties of chitosan-silica nanocomposite prepared by sol-gel method. *Nanoscale Res. Lett.* **2015**, *10*, No. 87.
(49) Akmaz, S.; Adiguzel, E. D.; Yasar, M.; Erguven, O. The effect of Ag content of the chitosan-silver nanoparticle composite material on the structure and antibacterial activity. *Adv. Mater. Sci. Eng.* **2013**, No. 690918.
(50) Chen, C. H.; Lin, Y. C.; Mao, C. F.; Liao, W. T. Green synthesis, size control, and antibacterial activity of silver nanoparticles on chitosan films. *Res. Chem. Intermed.* **2019**, *45*, 4463−4472.
(51) Kaur, P.; Duhan, J. S.; Thakur, R. Comparative pot studies of chitosan and chitosan-metal nanocomposites as nano-agrochemicals against fusarium wilt of chickpea (*Cicer arietinum* L.). *Biocatal. Agric. Biotechnol.* **2018**, *14*, 466−471.
(52) Dananjaya, S. H. S.; Erandani, W. K. C. U.; Kim, C. H.; Nikapitiya, C.; Lee, J.; Zoysa, M. D. Comparative study on antifungal activities of chitosan nanoparticles and chitosan silver nano composites against *Fusarium oxysporum* species complex. *Int. J. Biol. Macromol.* **2017**, *105*, 478−488.
(53) Shaikh, T.; Dalvi, S. G.; Suprasanna, P.; Pawar, B. H. In *Effect of Chitosan−Silver Nano-composite with Trichoderma viridae on Ceratocystis paradoxa*, Proceedings of 75th Annual Convention of Sugar Technologist Association of India (STAI), Calcutta West Bengal, India, July 17−19, 2019.

https://doi.org/10.1021/acsomega.1c05358
ACS Omega 2021, 6, 34812−34822